ELSEVIER

Carbohydrate Research 280 (1996) 1–14

CARBOHYDRATE RESEARCH

Structure of the saponin adjuvant QS-21 and its base-catalyzed isomerization product by ^{1}H and natural abundance ^{13}C NMR spectroscopy

Neil E. Jacobsen [a,*], Wayne J. Fairbrother [a], Charlotte R. Kensil [b], Amy Lim [a], Deborah A. Wheeler [b,1], Michael F. Powell [a]

[a] *Genentech, Inc., South San Francisco, CA 94080, USA*
[b] *Cambridge Biotech Corporation, Worcester, MA 01605, USA*

Received 18 April 1995; accepted in revised form 5 July 1995

Abstract

The saponin QS-21, derived from the bark of the *Quillaja saponaria* Molina tree, has shown great potential as an adjuvant with a number of vaccines. Kinetic studies carried out to establish the stability of vaccine formulations show that commercially supplied QS-21 (primarily QS-21A) is converted slowly at pH 5.5, and rapidly at higher pH, to an equilibrium mixture of two regioisomers, QS-21A and QS-21B, in a ratio of 20:1. NMR studies show that QS-21A and QS-21B differ only in the point of attachment of the fatty acyl moiety to the fucose sugar ring. The major isomer, QS-21A, has the fatty acyl portion attached at the 4-hydroxyl group whereas the minor isomer, QS-21B, has the fatty acyl portion attached at the 3-hydroxyl group. The isomerization most likely involves ionization of the 3-hydroxy group and intramolecular acyl transfer from the 4-hydroxy group. The relative stereochemistry of the triterpene and the sugar anomeric centers is also established by NMR methods.

Keywords: Saponin adjuvant, QS-21; Isomerization; Kinetics; NMR spectroscopy

1. Introduction

The development of a successful vaccine formulation for subunit antigens, such as HIV-1 gp120, requires the use of a potent adjuvant that induces both humoral and

* Corresponding author. Present address: Department of Chemistry, University of Arizona, Tucson, AZ 85721, USA.

[1] Formerly D.A. Bedore.

SSDI 0008-6215(95)00278-2

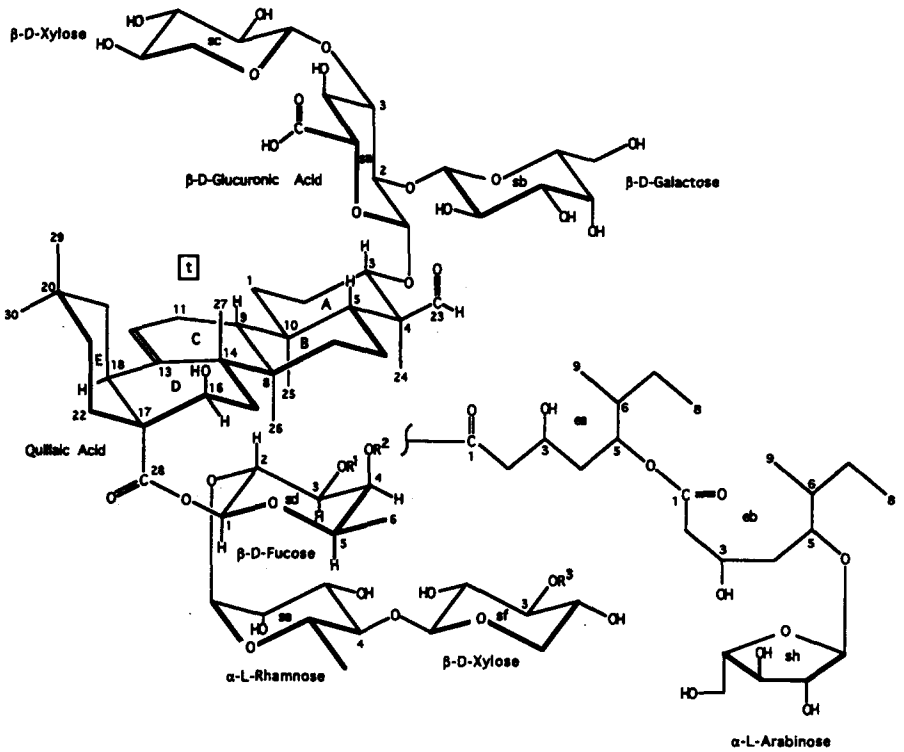

QS-21A: R^1 = H, R^2 = ea-eb-sh; QS21B: R^1 = ea-eb-sh, R^2 = H

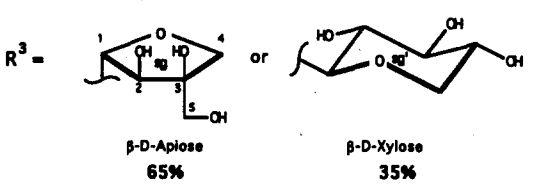

Fig. 1. Structure of QS-21A and QS-21B with the carbon numbering system shown. Absolute stereochemistry of the sugars is based on the most abundant enantiomer occurring in nature. The sugar heterogeneity for R^3 is the same for both QS-21A and QS-21B.

cell-mediated immune responses. QS-21, a saponin adjuvant derived from the bark of the *Quillaja saponaria* Molina tree, stimulates antigen-specific antibody and cytotoxic T lymphocyte responses to subunit antigen vaccines in mice [1,2]. QS-21 has previously been used with a cancer vaccine in humans [3], as well as in HIV-1 vaccine studies in non-human primates [4]. A structure was proposed for QS-21 based on mass spectrometry, degradation, and carbohydrate linkage analyses [5]. The structure (Fig. 1, QS-21B) consists of quillaic acid, a steroid-like triterpene, with one branched trisaccharide and

Table 1
Chemical shift assignments for QS-21A and QS-21B

No.	QS-21A		QS-21B	
	^{1}H [a] (ppm)	^{13}C [b] (ppm)	^{1}H [a] (ppm)	^{13}C [b] (ppm)
*t*1	**1.06, 1.65**	40.3	**1.06, 1.66**	40.3
*t*2	**1.90, 1.70**	26.8	**1.90, 1.73**	26.8
*t*3	3.88	87.2	3.89	87.2
*t*4	—	57.9	—	57.8
*t*5	1.30	49.9	1.30	49.9
*t*6	**0.80, 1.42**	22.6	**0.81, 1.43**	22.5
*t*7	**1.46, 1.23**	34.5	**1.46, 1.23**	34.5
*t*8	—	42.2	—	42.1
*t*9	1.65	48.9	1.66	48.9
*t*10	—	38.2	—	38.1
*t*11	1.86	25.7	1.86	25.7
*t*12	5.33	124.9	5.34	125.0
*t*13	—	145.3	—	145.3
*t*14	—	43.9	—	43.8
*t*15	**1.38, 1.58**	37.4	**1.39, 1.55**	37.4
*t*16	4.36	76.0	4.39	75.6
*t*17	—	51.5	—	51.4
*t*18	2.87	43.4	2.89	43.4
*t*19	**2.15, 1.04**	49.1	**2.15, 1.05**	49.1
*t*20	—	32.5	—	32.3
*t*21	**1.72, 1.17**	37.5	**1.71, 1.18**	37.4
*t*22	**1.85, 1.72**	32.6	**1.87, 1.71**	32.7
*t*23	9.36	213.6	9.37	213.5
*t*24	1.08	12.1	1.08	12.1
*t*25	0.93	18.0	0.94	17.8
*t*26	0.70	19.3	0.68	19.2
*t*27	1.29	28.7	1.30	28.7
*t*28	—	178.9	—	178.5
*t*29	0.85	34.7	0.85	34.7
*t*30	0.90	26.5	0.90	26.3
*ea*1	—	175.0	—	174.3
*ea*2	2.60, 2.60	44.9	2.63, 2.51	44.8
*ea*3	3.94	67.3	3.98	67.2
*ea*4	1.77, 1.66	40.5	1.77, 1.63	40.5
*ea*5	5.05	77.2	5.06	77.3
*ea*6	1.56	41.0	1.56	41.0
*ea*7	1.38, 1.09	27.6	1.38, 1.09	27.6
*ea*8	0.84	13.8	0.84	13.7
*ea*9	0.86	16.4	0.86	16.2
*eb*1	—	175.7	—	175.8
*eb*2	2.50, 2.50	45.2	2.53, 2.53	45.2
*eb*3	4.16	67.4	4.18	67.5
*eb*4	1.52, 1.50	40.1	1.57, 1.51	40.2
*eb*5	3.70	80.9	3.71	81.1
*eb*6	1.57	40.2	1.59	40.2
*eb*7	1.47, 1.02	26.5	1.48, 1.04	26.5
*eb*8	0.85	14.1	0.86	14.1
*eb*9	0.82	16.9	0.83	16.9

Table 1 (continued)

No.	QS-21A		QS-21B	
	^{1}H [a] (ppm)	^{13}C [b] (ppm)	^{1}H [a] (ppm)	^{13}C [b] (ppm)
*sa*1	4.38	104.9	4.40	104.9
*sa*2	3.61	79.2	3.62	79.2
*sa*3	3.70	86.6	3.72	86.6
*sa*4	3.47	72.9	3.50	72.3
*sa*5	3.63	78.7	3.69	78.7
*sb*1	4.67	104.6	4.68	104.6
*sb*2	3.37	74.2	3.37	74.2
*sb*3	3.48	75.8	3.49	75.8
*sb*4	3.78	71.9	3.79	71.8
*sb*5	3.49	77.9	3.49	77.9
*sb*6	3.70, 3.62	63.6	3.74, 3.64	63.7
*sc*1	4.57	105.4	4.57	105.4
*sc*2	3.22	76.0	3.23	76.0
*sc*3	3.33	78.5	3.34	78.5
*sc*4	3.52	71.8	3.53	71.8
*sc*5	**3.19, 3.88**	67.9	**3.20, 3.89**	67.8
*sd*1	5.33	96.1	5.39	96.0
*sd*2	3.67	77.0	3.96	73.9
*sd*3	3.90	75.1	4.92	79.2
*sd*4	5.06	76.6	3.80	71.3
*sd*5	3.83	72.3	3.77	73.7
*sd*6	1.00	18.1	1.12	17.9
*se*1	5.16	102.4	4.96	102.3
*se*2	3.88	72.7	3.74	72.5
*se*3	3.76	73.1	3.66	73.1
*se*4	3.48	85.0	3.49	84.9
*se*5	3.67	70.2	3.63	70.4
*se*6	1.23	19.8	1.24	19.8
*sf*1	4.51	107.5	4.50	107.5
*sf*2	3.27	76.5	3.27	76.5
*sf*3	3.43	86.0	3.44	86.0
*sf*4	3.50	70.6	3.50	70.6
*sf*5	**3.22, 3.85**	67.7	**3.22, 3.85**	67.6
*sg*1	5.19	111.7	5.20	111.7
*sg*2	3.96	79.4	3.97	79.4
*sg*3	—	82.0	—	81.9
*sg*4	4.05, 3.79	76.1	4.07, 3.80	76.1
*sg*5	3.60	66.2	3.61	66.3
*sh*1	4.97	109.2	4.99	109.3
*sh*2	3.95	84.1	3.96	84.0
*sh*3	3.83	78.8	3.84	78.8
*sh*4	3.96	85.9	3.97	86.0
*sh*5	3.70, 3.60	63.7	3.71, 3.60	63.8
*se'*1	5.13	102.5	4.94	102.4
*sf'*1	4.53	107.2	4.52	107.2
*sf'*2	3.33	76.2	3.33	76.0
*sf'*3	3.53	87.6	3.53	87.6
*sf'*4	3.55	70.4	3.53	70.4
*sf'*5	3.23, 3.89	—	3.24, 3.91	—

Table 1 (continued)

No.	QS-21A		QS-21B	
	^{1}H [a] (ppm)	^{13}C [b] (ppm)	^{1}H [a] (ppm)	^{13}C [b] (ppm)
*sg'*1	4.51	106.2	4.52	106.2
*sg'*2	3.28	76.0	3.30	76.2
*sg'*3	3.37	78.3	3.37	78.3
*sg'*5	—	—	3.20, 3.82	—

[a] Chemical shifts are referenced to external sodium 3-trimethylsilyl-propanoate-2,2,3,3-d_4 (TSP) as 0 ppm for ^{1}H and ^{13}C. Boldface indicates stereospecific assignments; in these cases the α shift is reported first. Protons that are *cis* to the aldehyde in the triterpene ring system are designated α, and protons *cis* to the acid are designated β; xylose 5-protons are designated α for axial and β for equatorial. Underline indicates an absolute value chemical shift difference greater than 0.08 ppm between QS-21A and QS-21B.

[b] Underline indicates an absolute value chemical shift difference of 0.4 ppm or greater between QS-21A and QS-21B. Comparison of QS-21B ^{13}C chemical shifts with the QS-17 aglycone in pyridine [6] shows significant differences (absolute value greater than 1.5 ppm relative to an apparent 2 ppm reference offset) in the triterpene near the points of chemical modification (*t*2, *t*3, *t*4, *t*10, *t*23, *t*24, *t*25), at the points of attachment of the two additional sugars (*se*3 and *sh*2), at the rhamnose anomeric carbon (*se*1), and in the fucose ring (*sd*3 and *sd*5). For QS-21A additional differences are observed for *sd*2 and *sd*4.

one unbranched tetrasaccharide attached, and a dimeric fatty acyl group attached to the first sugar of the tetrasaccharide by an ester linkage. An eighth sugar is attached to the fatty acyl group. The attachment of the fatty acyl moiety at the 3-hydroxyl group of the fucose ring and the stereochemistry of the triterpene and sugars were assigned by analogy to the related saponin QS-17, which was studied by ^{13}C NMR of degradation products [6]. The structure and stereochemistry of quillaic acid were established by 1D ^{1}H NMR studies and X-ray crystallography of similar triterpene ring systems [7,8].

The commercial product QS-21, supplied by Cambridge Biotech, is a dry white powder. Upon dissolution as a 2 mg/mL solution in 30% acetonitrile – 70% water, it elutes as a single predominant peak (designated QS-21A) when analyzed by reverse-phase HPLC (RP-HPLC). However, studies assessing the degradation of QS-21 have revealed the rapid initial formation of a second minor peak, QS-21B, in a ratio of about 20 to 1 (QS21A to QS21B) [9]. The peaks were separated, quantitated by RP-HPLC, and analyzed by fast atom bombardment mass spectroscopy. The mass spectral data suggested that these two peaks were isomers. It was also noted that QS-21B would rapidly reconvert into QS-21A, suggesting an equilibrium. In order to understand this equilibrium, we undertook kinetic and NMR studies of this transformation.

2. Results

Equilibration and separation of QS-21 isomers.—Incubation of QS-21 in aqueous solution at pH 5.5 results in a pseudo-first-order reaction that affords a 20:1 mixture of QS-21A and QS-21B after final equilibrium is reached (Fig. 2). The significantly shorter retention time of QS-21B relative to QS-21A in RP-HPLC permits a complete separation of the two isomers. The half-lives for reversion of purified QS-21B to the

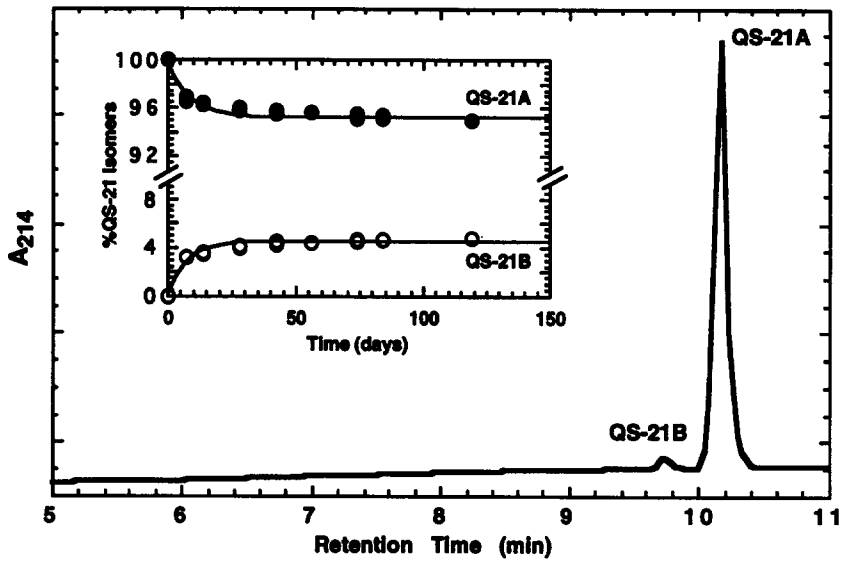

Fig. 2. Analytical RP-HPLC chromatogram (0.46 cm i.d.×25 cm YMC C4 column, linear gradient of 25–75% acetonitrile in water (0.1% TFA throughout) over a 15 min period with a flow rate of 1 mL/min) showing the shorter retention time of QS-21B relative to QS-21A. The inset shows the kinetics obtained when QS-21A (0.5 mg/mL) is incubated in pH 5.5 aqueous buffer (20 mM sodium succinate, 120 mM NaCl) at 5°C, with the formation of QS-21B. The curves result from a three-coefficient exponential fit which gives half-lives of 6.4 and 5.3 days for QS-21A and QS-21B, respectively.

equilibrium mixture at 22°C are 25, 2.3, and 1.0 days at pH 5.0, 6.0, and 7.0, respectively (data not shown).

NMR assignments.—The carbon atoms of QS-21 are designated as triterpene (*t*), fatty acid (*ea* and *eb*), and sugar (*sa-sh*), followed by the carbon number within each subunit. Protons that are *cis* to the aldehyde in the triterpene ring system are designated α, and protons *cis* to the acid are designated β; xylose 5-protons are designated α for axial and β for equatorial; and methylene protons that are not stereospecifically assigned are designated a (downfield) and b (upfield). Examination of the QS-21 structure (Fig. 1) shows that two of the singly hydroxylated carbons are esterified, leading to an expected downfield shift of ca. 1.35 ppm for the proton attached to that carbon [10]. Thus, the two non-anomeric downfield-shifted proton signals observed in the {^{13}C–^{1}H} HMQC spectra of both QS-21A and QS-21B (Fig. 3) can be assigned to the esterified non-anomeric carbon in the fucose sugar and the *ea*5 carbon of the fatty acyl moiety. Of these two signals, the *ea*5 signal can be identified by HMBC correlation to protons *ea*4, *ea*7a, *ea*7b, and *ea*9 and carbon *eb*1. The remaining esterified carbon correlates to fucose sugar ring protons. All of the carbons of both isomers can be assigned using these two carbons and the *t*23 and *t*12 carbons as starting points; the homonuclear TOCSY, COSY, and ROESY data provide confirmation. Complete ^{1}H and ^{13}C chemical shift assignments for both isomers are given in Table 1. The observed $^{1}J_{CH}$ coupling constants for QS-21A fell in the expected ranges [11] depending on the number

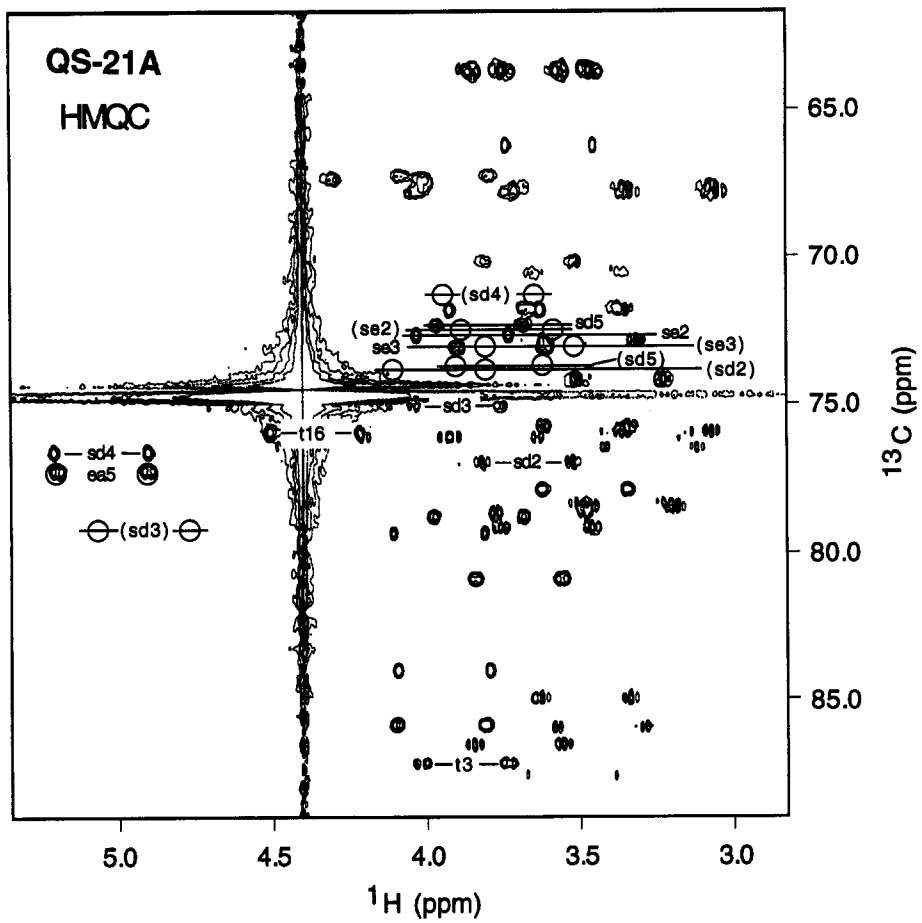

Fig. 3. HMQC spectrum of QS-21A showing the alcohol region. Because no ^{13}C decoupling was used during acquisition, each carbon gives a pair of cross-peaks separated by $^{1}J_{CH}$ in F_2. Circles indicate the position of cross-peaks observed in the corresponding QS-21B spectrum, which differ significantly in chemical shift from QS-21A. QS-21B assignments for these resonances are shown in parentheses.

of bonds to oxygen (mean ± standard deviation): 124 ± 4 Hz for 41 carbons with no bonds to oxygen; 146 ± 4 Hz for 41 carbons with one bond to oxygen; 170 ± 5 Hz for 9 carbons with two bonds to oxygen(s); and 152 Hz for the single olefinic carbon *t*12. The $^{1}J_{CH}$ values for the anomeric protons of QS-21A are: 163 (*sa*), 166 (*sb*), 165 (*sc*), 168.5 (*sd*), 174.5 (*se*), 162.5 (*sf*), 176.5 (*sg*), and 173.5 (*sh*). Similar values were observed for QS-21B. Heterogeneity is observed in the NMR data for the terminal sugar (*sg*) of the unbranched tetrasaccharide. This is consistent with degradation studies that show an ca. 2:1 mixture of apiose and xylose in this position [12] and does not affect the conclusions of the present study.

Assignment of the esterified non-anomeric fucose carbon was made using the HMBC spectra (Fig. 4), that correlate protons to carbon nuclei two or three bonds away. In

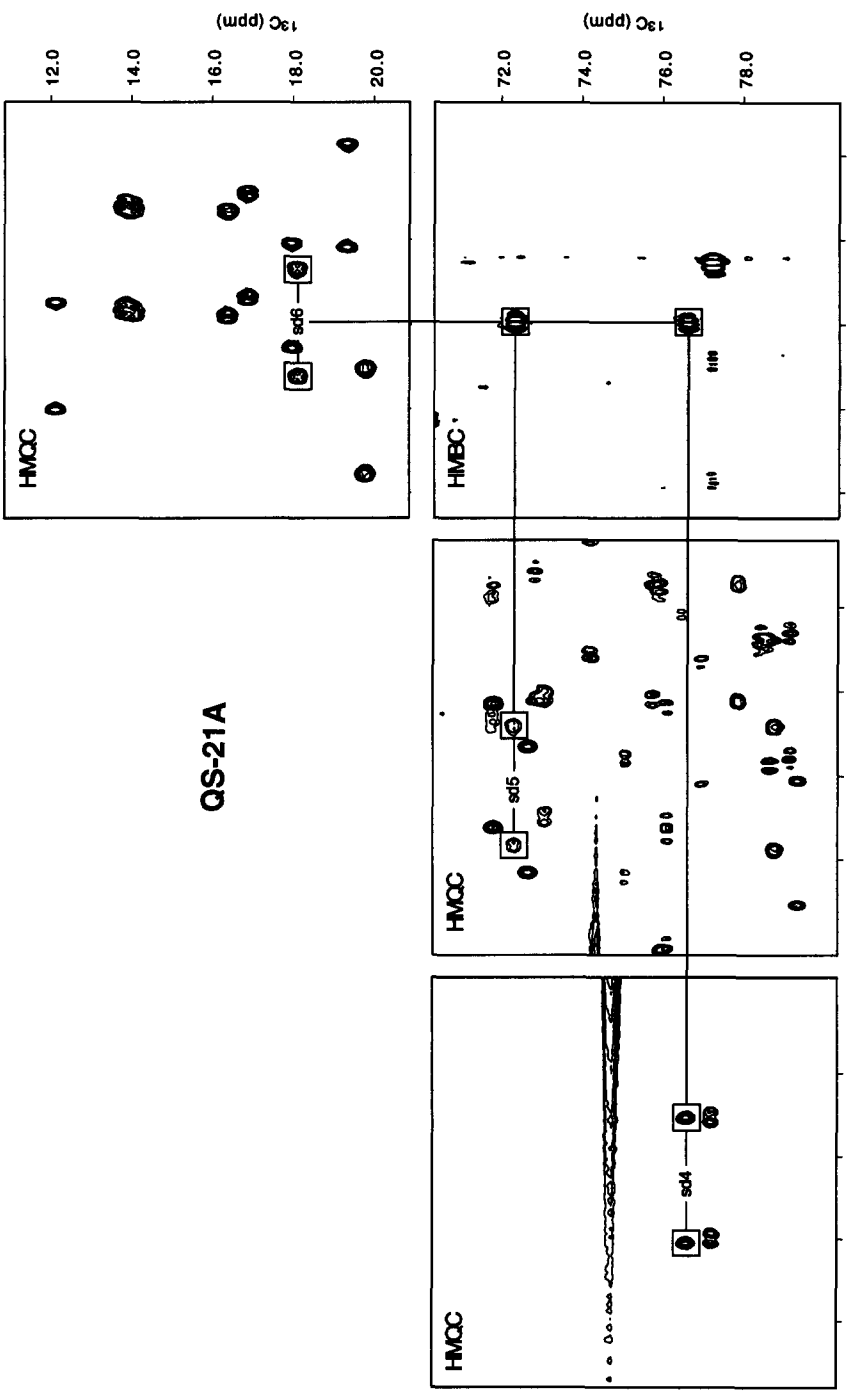

Fig. 4. HMBC spectrum of QS-21A (lower right) aligned with selected portions of the QS-21A HMQC spectrum, showing correlation of the fucose methyl protons (*sd6*) with C-4 and C-5 of the fucose ring.

QS-21A, but not in QS-21B, this carbon shows a strong correlation to the *sd*6 protons, which is possible for the *sd*4 carbon but not for the *sd*3 carbon. The homonuclear TOCSY spectra show similar patterns, with the downfield-shifted non-anomeric proton correlated to the *sd*6 methyl protons in QS-21A, but not in QS-21B; in QS-21B the downfield-shifted resonance shows a much stronger correlation to the anomeric proton (data not shown). Thus, the esterified carbon can be assigned to *sd*4 in QS-21A and *sd*3 in QS-21B. In the ROESY spectra, both isomers show NOE interactions from the *sd*6 methyl protons to the *sd*5 and *sd*4 ring protons, but not to the *sd*3 proton, which is downfield shifted in QS-21B (data not shown). The fucose ring assignments are confirmed by DQF-COSY cross-peaks for all vicinal pairs in both isomers.

Further confirmation of these assignments is obtained from coupling constant data. The esterified non-anomeric carbon on the fucose ring does not show resolved passive $^{1}H-^{1}H$ coupling in the HMQC spectrum for QS-21A (Fig. 3), but a large (ca. 9 Hz)

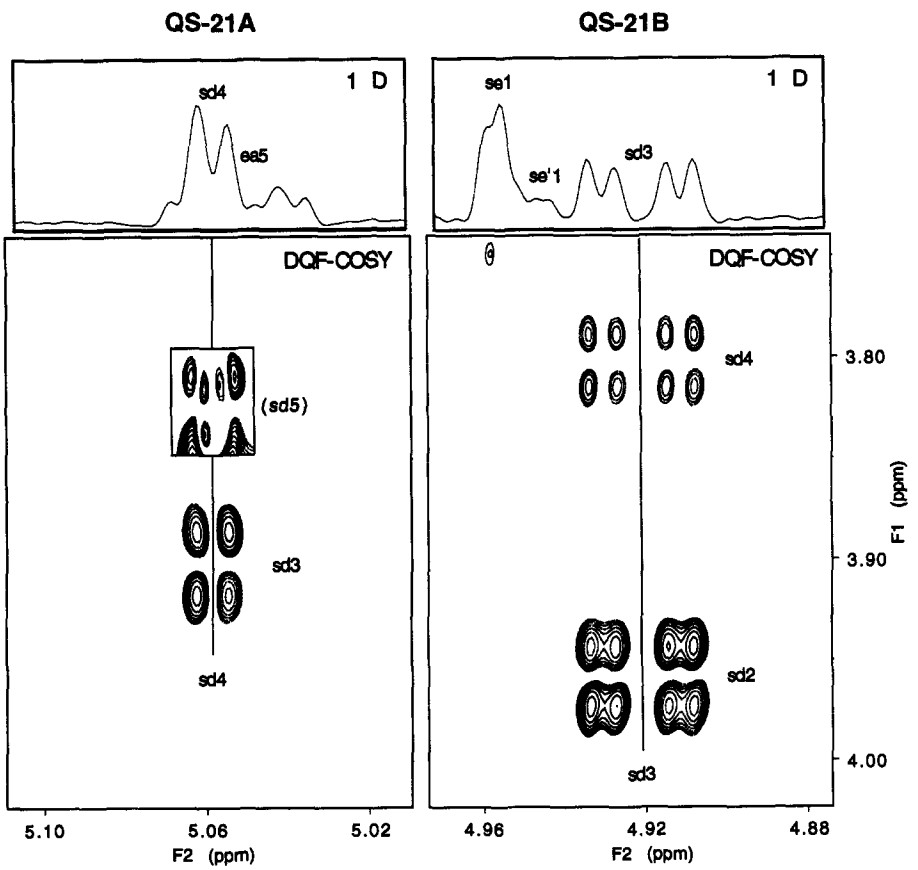

Fig. 5. Expanded regions of the DQF-COSY spectra of QS-21A and QS-21B, with the portion of the 1D spectrum corresponding to the F_2 region. The weak QS-21A *sd*5-*sd*4 cross-peak (box) is shown at a contour level a factor of 7 lower.

coupling is observed for QS-21B. The homonuclear DQF-COSY spectra (Fig. 5) show a large coupling (9.4 Hz) and a small coupling (3.4 Hz) for the downfield-shifted fucose proton in QS-21B, but only one fully resolved coupling (3.7 Hz) for this resonance in QS-21A. The QS-21B pattern is consistent with the expected coupling constants for the *sd*3 proton: one large (axial–axial) coupling to the *sd*2 proton and one small (axial–equatorial) coupling to the equatorial *sd*4 proton (Fig. 1). In contrast, QS-21A has the fatty acyl (*ea-eb-sh*) group attached at carbon 4 of the fucose moiety, consistent with the absence of a large (axial–axial) $^{1}H-^{1}H$ coupling constant for the downfield-shifted fucose proton. By comparison, in methyl β-D-fucopyranoside the H-3 resonance exhibits couplings of 10.0 and 3.6 Hz and the H-4 resonance has couplings of 3.6 and 0.8 Hz [13].

The observed difference in the point of attachment of the fatty acyl moiety is the only structural difference between the two isomers. The significant chemical shift differences between QS-21A and QS-21B are limited to a few resonances in and around the fucose sugar moiety (Fig. 3 and underlined shifts in Table 1): *t*28, *sd*2-6, *se*1-3, *ea*1, and *ea*2.

Points of attachment of subunits.—The connectivity of the sugar, fatty acyl, and triterpene moieties was confirmed by NMR methods. One or both three-bond HMBC connectivities are observed spanning each glycosidic linkage, and NOE interactions are generally observed from the anomeric proton to the linked sugar at the point of attachment and at the two adjacent positions. In both isomers, the fucose anomeric proton shows an HMBC correlation to the *t*28 carbonyl carbon and the downfield-shifted non-anomeric fucose proton is correlated to the *ea*1 carbonyl carbon.

Triterpene stereochemistry.—The relative stereochemistry of the triterpene moiety was confirmed by HMBC and NOE interactions. Strong three-bond HMBC correlations from the *t*5 and *t*9 protons to the *t*25 methyl carbon, and from the *t*9 proton to the *t*26 methyl carbon, confirm the *trans*-anti-*trans* stereochemistry of rings A, B, and C (Fig. 1). Such three-bond correlations are either absent or very weak for *gauche* relationships, as predicted by the Karplus relation [14,15]. In addition, long-range COSY cross-peaks are observed from the *t*26 methyl protons to the *t*9, *t*7α, and *t*27 protons. The *t*27 methyl protons have a strong NOE cross-peak to *t*19α and a weak cross-peak to *t*18, indicating that the *t*18 proton is *trans* to the *t*27 methyl group. The strong HMBC cross-peaks from *t*22α and *t*22β protons to *t*20 and *t*16 carbons, respectively, place the *t*17–*t*16 bond axially on ring E. The DE ring junction must be *cis* because the *t*18 proton is axial to ring E (a HMBC cross-peak is not observed to the *t*20 carbon and $^{3}J_{HH}$ for *t*18–*t*19α is 14.5 Hz). The *t*24 methyl group is axial in ring A (a strong three-bond HMBC cross-peak is observed to the *t*5 proton) and the *t*3 oxygen is equatorial (a strong three-bond HMBC cross-peak is observed from the *t*3 proton to the *t*24 carbon and the *t*3–*t*2β $^{3}J_{HH}$ is 11.6 Hz). The *t*16 hydroxyl is axial on ring D (a strong three-bond HMBC cross-peak is observed from the *t*16 proton to the *t*14 carbon). The stereospecific methylene and methyl group assignments in Table 1 are based on similar arguments.

Carbohydrate stereochemistry.—The anomeric configurations of the pyranose sugars can be established easily by NMR. For QS-21A the $^{3}J_{H\text{-}1,H\text{-}2}$ values are as follows (in Hz): 7.7 (*sa*), 7.7 (*sb*), 7.8 (*sc*), 8.0 (*sd*), 2.0 (*se*), 7.8 (*sf*), 3.2 (*sg*), and 2.2 (*sh*). Essentially identical values are obtained for QS-21B. Thus, for the pyranoses the

anomeric oxygen is equatorial (β configuration) in sugars *a*, *b*, *c*, *d*, and *f* and axial (α configuration) in sugar *e*. The corresponding methyl glycosides in D_2O have $^3J_{H\text{-}1,H\text{-}2}$ values (in Hz) of 8.0 (*sb*), 7.8 (*sc*, *sf*), 8.2 (*sd*), and 1.6 (*se*) [13]. Of the pyranose sugars, only the rhamnose unit (sugar *e*) shows three-bond HMBC cross-peaks from the anomeric proton to C-3 and C-5, confirming that this sugar has the α configuration (H-1 equatorial). This is consistent with the weak H-1–H-3 and H-1–H-5 ROESY cross-peaks and the large anomeric $^1J_{CH}$ values [15] observed for sugar *e* in both QS-21 isomers. The configuration of sugar *g* (apiose) is assigned as β by comparison of its anomeric carbon ^{13}C chemical shift (111.7 ppm in both isomers) with the methyl apiofuranosides (α: 104.4 ppm; β: 111.3 ppm) [16]. This is supported by the very weak H-1–H-5 NOE, that is barely detectable in QS-21A and is not observed in the more dilute QS-21B sample. The ^{13}C chemical shifts of sugar *h* (arabinose) in QS-21A and QS-21B closely match those of methyl α-arabinofuranoside [13].

Commercial QS-21.—The 1D ^1H NMR spectrum of commercial QS-21 was essentially identical to that of QS-21A, with no detectable amount of QS-21B. This is consistent with RP-HPLC analysis of commercial QS-21, which indicated the presence of only QS-21A when assayed immediately after solubilization.

3. Discussion

QS-21A and its base-catalyzed isomerization product, QS-21B, differ only in the position of attachment of the fatty acid (*ea-eb-sh*) moiety to the fucose (*sd*) sugar moiety by an ester linkage. QS-21B, the minor isomer resulting from base-catalyzed isomerization of the commercial product QS-21, has the structure previously published for QS-21 [5], whereas QS-21A has the fatty acyl group attached to the axial C-4

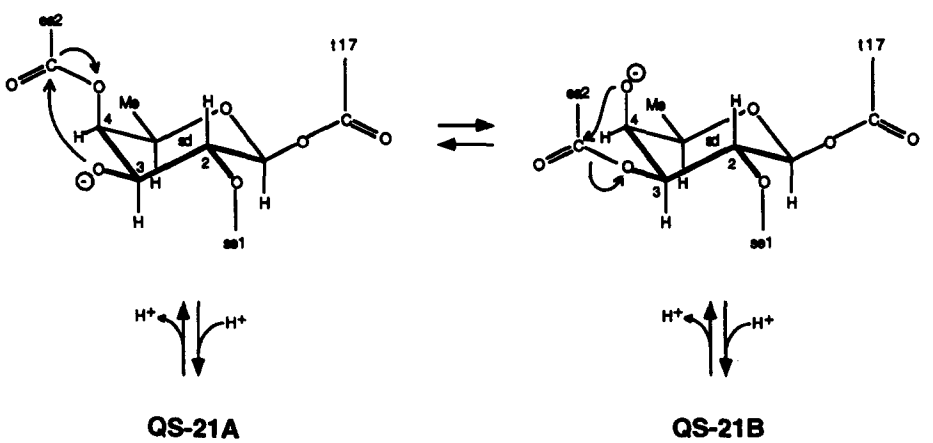

Fig. 6. Fucose ring portion of the structure of QS-21, showing the proposed mechanism for base-catalyzed isomerization.

hydroxyl. The two isomers appear to be equally active as adjuvants, but the possibility of rapid in vivo interconversion of isomers has not been ruled out [9].

Trans-esterification of the fatty acyl group (*ea-eb-sh*) between the *cis*-related hydroxyls on C-3 and C-4 of the fucose moiety appears to be an accessible base-catalyzed process, allowed by Baldwin's rules [17]. The proposed mechanism for the isomerization reaction (Fig. 6) involves deprotonation of the *sd*3 hydroxyl group of QS-21A followed by nucleophilic attack on the ester carbonyl group and acyl transfer from the *sd*4 hydroxyl to the *sd*3 hydroxyl. Protonation of the leaving group anion on *sd*4 then gives QS-21B. An alternative mechanism involving attack of the neutral hydroxyl oxygen on the ester carbonyl group without prior deprotonation could also be important at neutral and lower pH. Why the thermodynamically more stable isomer has the fatty acyl group in the axial (*sd*4) position is unclear, but this could be controlled by the overall conformation and aggregation state of the molecule.

The stereochemistry of the triterpene moiety is *trans*-anti-*trans*-anti-anti-*cis*, as shown in Fig. 1, with the 3-hydroxy group, the 24-methyl group, and the 16-proton *cis* to the 28-carboxy group. With the exceptions of rhamnose (*se*) and arabinose (*sh*), all of the sugars have the β-configuration.

4. Experimental

HPLC separation of QS-21A and QS-21B.—After equilibration of the QS-21 isomers at pH 5.5 (Fig. 2), semi-preparative RP-HPLC was carried out using a Vydac C4 column (2.5 cm i.d. × 25 cm) and a linear gradient of 30–45% acetonitrile in water (0.15% TFA throughout) over a 30 min period at a flow rate of 7.5 mL/min. Alternatively, 0.2 mg/mL QS-21 (Cambridge Biotech) was incubated in 100 mM ammonium bicarbonate (pH 7.8) for 20 min at 60°C and then acidified with 1 N acetic acid to 100 mM. This preparation (approximate ratio of QS-21A to QS-21B of 8:1) was lyophilized, redissolved in 25% acetonitrile to 8 mg/mL, and purified by RP-HPLC on Vydac C4 (5 μm, 1.0 cm i.d. × 25 cm), using a linear gradient of 25–45% acetonitrile in water (0.15% TFA throughout) over a 60 min period at a flow rate of 3.0 mL/min. The fractions corresponding to pure QS-21A and QS-21B were lyophilized to dryness.

Kinetics of isomerization.—Pure, lyophilized samples of QS-21A and QS-21B were reconstituted in aqueous buffer (0.5 mg/mL at pH 5.5, 5°C or 200 μg/mL at pH 5.0, 6.0, or 7.0 at 22°C) for kinetic analysis. Briefly, aliquots were removed at known time intervals and analyzed by RP-HPLC using UV detection at 214 nm. The peak areas were integrated and kinetic curves were generated directly from the integrals, assuming the integrals at zero time represent 100% of the QS-21 (QS-21A plus QS-21B).

Nuclear magnetic resonance (NMR) spectroscopy.—Dry, lyophilized samples of QS-21A (3 mg), QS-21B (1.5 mg), and commercial QS-21 from Cambridge Biotech Corp. (1.8 mg) were each dissolved in 0.50 mL of a 70:30 (v/v) mixture of acidified D_2O (brought to pH 4 by addition of acetic acid-d_4) and acetonitrile-d_3. The use of the organic co-solvent was dictated by the low water solubility of QS-21 at low pH and by the formation of micelles (critical micellar concentration = 24 μM) in pure water. After

collection of all NMR data, the QS-21A and QS-21B samples were analyzed by RP-HPLC: sample QS-21A was 6 mg/mL of 95% QS-21A and 5% QS-21B and sample QS-21B was 2.9 mg/mL of 90% QS-21B and 10% QS-21A. The QS-21A fucose ring resonances were clearly identified as minor cross-peaks in the QS-21B homonuclear 2D spectra.

NMR spectra were acquired on a Bruker AMX-500 NMR spectrometer with a proton frequency of 500 MHz and a 5 mm triple-resonance inverse $^{1}H/^{15}N/^{13}C$ probe. All spectra were acquired at 30°C without spinning, with presaturation of the residual water signal. One-dimensional proton spectra were acquired with a spectral width of 12 500 Hz using a Hahn spin-echo before acquisition [18,19]. Unless otherwise indicated, all 2D spectra were acquired in the phase-sensitive mode using time-proportional phase incrementation (TPPI) [20–22], with spectral widths of 12,500 Hz [23] in F_2 and 6250 Hz (homonuclear) or 16,340 Hz (heteronuclear) in F_1, acquiring 4096 complex points in t_2. The initial sampling delay was one dwell time, with a final t_1 delay of 60 ms and a total experiment time of 29 h. The data were zero-filled to 8192 complex points in t_2 and 2048 real points in t_1, right-shifted by one point in t_1, multiplied by a cosine-bell window in both dimensions and transformed into a 4096×1024 real matrix, discarding the first and last 2048 points in F_2.

Double-quantum filtered (DQF) COSY [24] spectra were acquired with a spectral width of 6250 Hz in F_2, and convolution difference [25] was used in F_2 to attenuate the solvent signal. An unshifted sine-bell window was used in both dimensions. For determination of J values, the same data were zero-filled to 16,384 points in both dimensions to increase digital resolution and provide more points for curve fitting, and no window function was used in t_2. The sum of about 10 rows along F_2 representing one lobe of a cross-peak was fitted to an antiphase Lorentzian doublet using the Levenberg–Marquardt algorithm [26]. Total correlation (TOCSY) [27,28] spectra were acquired using a clean-DIPSI [29] isotropic mixing sequence for 70 ms, with a Hahn spin-echo before acquisition. Rotating-frame NOE (ROESY) [30,31] spectra were acquired with a CW spin-lock field strength of 4500 Hz and a mixing time of 175 ms. The carrier was shifted after presaturation of the water resonance (4.41 ppm) to 3.00 ppm and the F_1 spectral width was narrowed to 2600 Hz, excluding the aldehyde resonance. The transformed matrix was baseline corrected using the FLATT method [32].

Natural abundance $\{^{13}C-^{1}H\}$ heteronuclear multiple-quantum correlation (HMQC) spectra [33,34] were acquired in the States [35] mode with delays of 3.4 ms for evolution and refocusing of antiphase magnetization, and a maximum t_1 value of 23 ms. The ^{13}C carrier was placed at 74.7 ppm and no ^{13}C decoupling was applied during acquisition. The initial sampling delay was set to 1.5 dwell times in t_1 so that the aliased peaks (carbonyl resonances) would appear with opposite phase. Natural abundance $\{^{13}C-^{1}H\}$ heteronuclear multiple-bond correlation (HMBC) spectra [36] were acquired similarly to the HMQC spectra except that the phase of the first ^{13}C pulse was alternated to cancel one-bond correlations and an additional 50 ms evolution time and ^{13}C $\pi/2$ pulse were added to allow multiple-bond antiphase magnetization to develop. Antiphase magnetization was not refocused prior to acquisition, so cross-peaks appear as antiphase doublets of random phase in F_2. The total experiment time was 44 h.

Acknowledgements

We thank Drs Jeffrey Cleland and Nicholas Skelton for support and advice in this project.

References

[1] C.R. Kensil, U. Patel, M. Lennick, and D. Marciani, *J. Immunol.*, 146 (1991) 431–437.
[2] M.J. Newman, J.-Y. Wu, B.H. Gardner, K.J. Munroe, D. Leombruno, J. Recchia, C.R. Kensil, and R.T. Coughlin, *J. Immunol.*, 148 (1992) 2357–2362.
[3] P.O. Livingston, S. Adluri, F. Helling, T.-J. Yao, C.R. Kensil, M.J. Newman, and D. Marciani, *Vaccine*, 12 (1994) 1275–1280.
[4] M.J. Newman, J.-Y. Wu, R.T. Coughlin, C.I. Murphy, J.R. Seals, M.S. Wyand, and C.R. Kensil, *AIDS Research and Human Retroviruses*, 8 (1992) 1413–1418.
[5] C.R. Kensil, S. Soltysik, U. Patel, and D.J. Marciani, in F. Brown, R.M. Chanock, H.S. Ginsberg, and R.A. Lerner (Eds.), *Vaccines '92: Modern Approaches to New Vaccines Including Prevention of AIDS*, Cold Spring Harbor Laboratory Press, 1992, pp 35–40.
[6] R. Higuchi, Y. Tokimitsu, and T. Komori, *Phytochemistry*, 27 (1988) 1165–1168.
[7] H.-D. Woitke, J.-P. Kayser, and K. Hiller, *Die Pharmazie*, 25 (1970) 133–143.
[8] W. Hoppe, A. Gieren, N. Brodherr, R. Tschesche, and G. Wulff, *Angew. Chem.*, 80 (1968) 563–564.
[9] J.L. Cleland, C.R. Kensil, A. Lim, N.E. Jacobsen, L. Basa, M. Spellman, D. Bedore, and M.F. Powell, *J. Pharm. Sci.*, 1995, in press.
[10] R.M. Silverstein, G.C. Bassler, and T.C. Morrill, *Spectrometric Identification of Organic Compounds*, Wiley, New York, 1981.
[11] E. Breitmaier and W. Voelter, *^{13}C NMR Spectroscopy*, Verlag Chemie, Weinheim, 1978.
[12] S. Soltysik, D.A. Bedore, and C. Kensil, *Ann. N.Y. Acad. Sci.*, 690 (1993) 392–395.
[13] K. Bock and H. Thøgersen, *Annu. Rep. NMR Spectrosc.*, 13 (1982) 1–57.
[14] V.F. Bystrov, *Prog. Nucl. Magn. Reson.*, 10 (1976) 41–81.
[15] R. Barker, H.A. Nunez, P. Rosevear, and A.S. Serianni, *Methods Enzymol.*, 83 (1982) 58–69.
[16] R. Higuchi, Y. Tokimitsu, T. Fujioka, T. Komori, T. Kawasaki, and D.G. Oakenful, *Phytochemistry*, 26 (1987) 229–235.
[17] J.E. Baldwin and M.J. Lusch, *Tetrahedron*, 38 (1982) 2939–2947.
[18] D.G. Davis, *J. Magn. Reson.*, 81 (1989) 603–607.
[19] M. Rance and R.A. Byrd, *J. Magn. Reson.*, 54 (1983) 221–240.
[20] R.L. Vold, R.R. Vold, R. Poupko, and G. Bodenhausen, *J. Magn. Reson.*, 38 (1980) 141–161.
[21] D. Marion and K. Wüthrich, *Biochem. Biophys. Res. Commun.*, 113 (1983) 967–974.
[22] A.G. Redfield and S.D. Kuntz, *J. Magn. Reson.*, 19 (1975) 250–254.
[23] M.A. Delsuc and J.Y. Lallemand, *J. Magn. Reson.*, 69 (1986) 504–507.
[24] M. Rance, O.W. Sørensen, G. Bodenhausen, G. Wagner, R.R. Ernst, and K. Wüthrich, *Biochem. Biophys. Res. Commun.*, 117 (1983) 479–485.
[25] D. Marion, M. Ikura, and A. Bax, *J. Magn. Reson.*, 84 (1989) 425–430.
[26] W.H. Press, B.P. Flannery, S.A. Teukolsky, and W.T. Vetterling, *Numerical Recipes: The Art of Scientific Computing*, Cambridge University Press, Cambridge, 1986.
[27] D.G. Davis and A. Bax, *J. Magn. Reson.*, 64 (1985) 533–535.
[28] L. Braunschweiler and R.R. Ernst, *J. Magn. Reson.*, 53 (1983) 521–528.
[29] J. Cavanagh and M. Rance, *J. Magn. Reson.*, 96 (1992) 670–678.
[30] B.T. Farmer II, S. Macura, and L.R. Brown, *J. Magn. Res.*, 80 (1988) 1–22.
[31] L.R. Brown and B.T. Farmer II, *Methods Enzymol.*, 176 (1989) 199–216.
[32] P. Güntert and K. Wüthrich, *J. Magn. Reson.*, 96 (1992) 403–407.
[33] L. Müller, *J. Am. Chem. Soc.*, 101 (1979) 4481–4484.
[34] A. Bax, R.H. Griffey, and B.L. Hawkins, *J. Magn. Reson.*, 55 (1983) 301–315.
[35] D.J. States, R.A. Haberkorn, and D.J. Ruben, *J. Magn. Reson.*, 48 (1982) 286–292.
[36] M.F. Summers, L.G. Marzilli, and A. Bax, *J. Am. Chem. Soc.*, 108 (1986) 4285–4294.